

# Individual low-energy E1 toroidal and compression states in light nuclei: deformation effect, spectroscopy and interpretation

V.O. Nesterenko<sup>1,2,3</sup>, J. Kvasil<sup>4</sup>, A. Repko<sup>5</sup>, and P.-G. Reinhard<sup>6</sup>

<sup>1</sup> *Laboratory of Theoretical Physics, Joint Institute for Nuclear Research, Dubna, Moscow region, 141980, Russia*

<sup>2</sup> *State University "Dubna", Dubna, Moscow Region, 141980, Russia*

<sup>3</sup> *Moscow Institute of Physics and Technology, Dolgoprudny, Moscow region, 141701, Russia*

<sup>4</sup> *Institute of Particle and Nuclear Physics, Charles University, CZ-18000, Praha 8, Czech Republic*

<sup>5</sup> *Institute of Physics, Slovak Academy of Sciences, 84511, Bratislava, Slovakia and*

<sup>6</sup> *Institut für Theoretische Physik II, Universität Erlangen, D-91058, Erlangen, Germany*

(Dated: December 15, 2024)

The existence of individual low-energy E1 toroidal and compression states (TS and CS) in  $^{24}\text{Mg}$  was predicted recently in the framework of quasiparticle random-phase-approximation (QRPA) model with Skyrme forces. It was shown that the strong axial deformation of  $^{24}\text{Mg}$  is crucial to downshift the toroidal strength to the low-energy region and thus make the TS the lowest E1( $K=1$ ) dipole state. In this study, we explain this result by simple mean-field arguments. Comparing TS in two strongly axial nuclei,  $^{24}\text{Mg}$  and  $^{20}\text{Ne}$ , we show that the lowest TS is not a universal phenomenon but rather a peculiarity of  $^{24}\text{Mg}$ . The spectroscopy of TS and CS is analyzed and some additional interpretation of these states is suggested.

## I. INTRODUCTION

In a recent publication [1], we have predicted the occurrence of individual low-energy E1 toroidal and compressional states (TS and CS) in  $^{24}\text{Mg}$ . The calculations were performed within the quasiparticle random-phase-approximation (QRPA) method using several Skyrme forces. This prediction opens a new promising path in exploration of toroidal excitations. Previously the nuclear toroidal mode was mainly studied in terms of the giant isoscalar ( $T=0$ ) toroidal dipole resonance (TDR), see e.g. [2–13] and references therein. However the experimental observation and identification of the TDR is plagued with serious troubles. The resonance is usually masked by other multipole modes (including dipole excitations of non-toroidal nature) located at the same energy region. As a result, even the most reliable ( $\alpha, \alpha'$ ) experimental data for E1( $T=0$ ) TDR [14, 15] can be disputed, see the detailed discussion in Ref. [13]. In this respect, the individual low-energy E1( $T=0$ ) TS in light nuclei have significant advantages. As shown [1], the TS in axially deformed  $^{24}\text{Mg}$  should appear as the lowest ( $E=7.92$  MeV) dipole state with  $K=1$  ( $K$  is the projection of the total angular momentum to the symmetry  $z$ -axis). It is well separated from the neighbouring dipole states, which simplifies its experimental identification and exploration as compared to the TDR. Low-energy TS were also predicted in other light deformed nuclei, see e.g. the AMD (antisymmetrized molecular dynamics) calculations for  $^{10}\text{Be}$  [16].

As demonstrated in [1], the TS in  $^{24}\text{Mg}$  becomes the lowest E1( $K=1$ ) state due to the large deformation-induced downshift of its excitation energy. So just the large axial quadrupole deformation makes the TS an individual mode, well separated from other states. This finding rises two questions. 1) How to explain this deformation effect by simple mean-field arguments? 2) How universal is this effect in strongly deformed light nuclei?

These questions are addressed in the present study where we compare the impact of deformation in two strongly deformed  $N=Z$  nuclei,  $^{24}\text{Mg}$  and  $^{20}\text{Ne}$ . For completeness, both vortical TS and irrotational CS are considered. It will be shown that the significant deformation-induced energy downshift is pertinent to both of  $^{24}\text{Mg}$  and  $^{20}\text{Ne}$ . However, in  $^{20}\text{Ne}$ , the TS is not the lowest dipole  $K=1$  state anymore. Moreover, in  $^{20}\text{Ne}$ , TS lies higher than CS. This means that  $^{24}\text{Mg}$  is perhaps rather unique light nucleus where the conditions for discrimination of the TS are most convenient.

Besides, we consider spectroscopic properties of TS and CS and suggest their interpretation in terms of low-energy  $T=0$  dipole states with isospin-forbidden E1 transition (for TS) and octupole mode (for CS).

## II. CALCULATION SCHEME

The calculations are performed within self-consistent QRPA based on the Skyrme functional [17]. We use the Skyrme parametrization SLy6 [18] as in the previous study [1]. The QRPA code for axial nuclei [19] exploits a 2D coordinate-space mesh in cylindrical coordinates. The single-particle spectrum is taken from the bottom of the potential well up to +55 MeV in the continuum. The equilibrium deformation is calculated by minimization of the total energy. Calculations with non-equilibrium deformations are performed using quadrupole constrained Hartree-Fock. The volume monopole pairing is treated at the BCS level [13]. The QRPA uses two-quasiparticle (2qp) basis with excitation energies up to  $\sim 100$  MeV. The basis includes  $\approx 1700$ – $1900$  ( $K=0$ ) and  $\approx 3200$ – $3600$  ( $K=1$ ) states. The Thomas-Reiche-Kuhn sum rule [20, 21] and isoscalar dipole energy-weighted sum rule [22] are exhausted by 100% and 97%, respectively.

Since vortical toroidal and irrotational compressional modes are coupled [7–9], we inspect both TS and CS.

The toroidal and compression dipole responses (reduced transition probabilities) are

$$B_\nu(E1K, \alpha) = (2 - \delta_{K,0}) |\langle \nu | \hat{M}_\alpha(E1K) | 0 \rangle|^2 \quad (1)$$

where  $|\nu\rangle$  is the wave function of the  $\nu$ -th QRPA dipole state. The toroidal ( $\alpha = \text{tor}$ ) and compressional ( $\alpha = \text{com}$ ) transition operators are [1, 9, 10]

$$\hat{M}_{\text{tor}}(E1K) = \frac{-1}{10\sqrt{2}c} \int d^3r r [r^2 + d^s + d_K^a] \mathbf{Y}_{11K} \cdot (\nabla \times \hat{\mathbf{j}}), \quad (2)$$

$$\hat{M}_{\text{com}}(E1K) = \frac{-i}{10c} \int d^3r r [r^2 + d^s - 2d_K^a] Y_{1K}(\nabla \cdot \hat{\mathbf{j}}), \quad (3)$$

where  $\hat{\mathbf{j}}(\mathbf{r})$  is operator of the nuclear current;  $\mathbf{Y}_{11K}(\hat{\mathbf{r}})$  and  $Y_{1K}(\hat{\mathbf{r}})$  are vector and ordinary spherical harmonics;  $d^s = -5/3\langle r^2 \rangle_0$  is the center-of-mass correction (c.m.c.) in spherical nuclei [9];  $d_K^a = \sqrt{4\pi/45}\langle r^2 Y_{20} \rangle_0(3\delta_{K,0} - 1)$  is the additional c.m.c. in axial deformed nuclei within the prescription [23]. The average values mean  $\langle f \rangle_0 = \int d^3r f \rho_0 / A$  where  $\rho_0$  is the g.s. density. We have checked that these c.m.c. accurately remove spurious admixtures.

The toroidal operator (2) with the curl  $\nabla \times \hat{\mathbf{j}}$  is vortical while the compression operator (3) with the divergence  $\nabla \cdot \hat{\mathbf{j}}$  is irrotational. Using the continuity equation, the current-dependent operator (3) can be transformed [9] to the familiar density-dependent form [22]  $\hat{M}'_{\text{com}}(E1K) = 1/10 \int d^3r \hat{\rho} [r^2 + d^s - 2d_K^a] Y_{1K}$  with  $\hat{\rho}(\mathbf{r})$  being the density operator.

The isoscalar ( $T=0$ ) nuclear current  $\hat{\mathbf{j}}$  includes the convection part  $\mathbf{j}_c^q$  (with effective charges  $e_{\text{eff}}^{\text{n},\text{p}} = 0.5$ ) and magnetization (spin) part  $\mathbf{j}_m^q$  (with g-factors  $g_s^{\text{n},\text{p}} = (\bar{g}_s^n + \bar{g}_s^p)\eta/2 = 0.88\eta$  where  $\bar{g}_s^{\text{n},\text{p}}$  are bare g-factors and  $\eta = 0.7$  is the quenching) [9].  $T=0$  responses are relevant when considering TS and CS in isoscalar reactions like  $(\alpha, \alpha')$ . The fields of the convection nuclear current are calculated as the current transition densities (CTD)  $\delta \mathbf{j}_c^q = \langle \nu | \hat{\mathbf{j}}_c^q | 0 \rangle$ .

### III. RESULTS AND DISCUSSION

#### A. $^{24}\text{Mg}$

First of all we recall the results [1] concerning the deformation-induced energy downshift for the toroidal and compressional responses in  $^{24}\text{Mg}$ . In figure 1, the responses (1) for  $K=1$  dipole states are depicted for different deformations [1], including the calculated equilibrium deformation  $\beta=0.536$  (which is rather close to the experimental value  $\beta_{\text{exp}}=0.605$ ). Figure 1 shows that increase of the deformation downshifts the toroidal strength yielding eventually a remarked toroidal state with energy 7.92 MeV, the lowest in the dipole spectrum. The compressional  $K=1$  strength which is much weaker than the toroidal one is also downshifted with increasing deformation. The plots e) and f) show that the 7.92 MeV state,

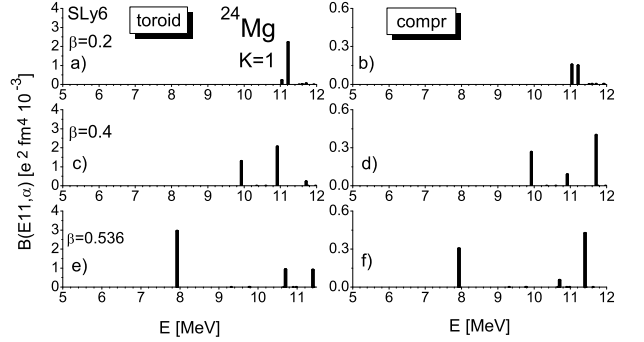


FIG. 1:  $T=0$  toroidal (left) and compression (right)  $B(E11)$ -responses for  $K=1$  states in  $^{24}\text{Mg}$ , calculated for deformations  $\beta=0.2$  (upper), 0.4 (middle), and equilibrium deformation 0.536 (bottom) [1]. Note different scales in the right and left plots.

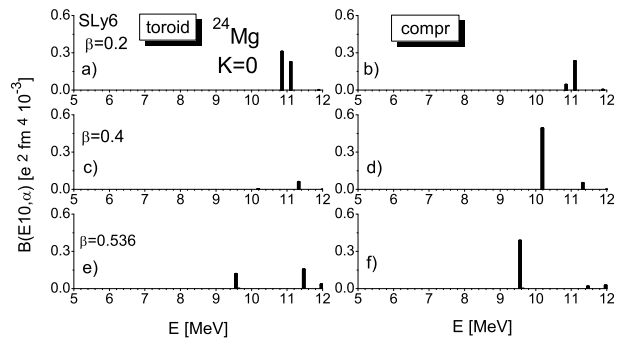


FIG. 2: The same in Fig. 1 but for  $K=0$  dipole states [1].

being mainly toroidal, has also a minor irrotational compression admixture.

Figure 2 exhibits similar responses for  $K=0$  states [1]. Here we see a definite downshift mainly for the compressional strength. At  $\beta=0.536$ , it yields a noticeable peak at 9.56 MeV, constituting the lowest  $K=0$  state. Being mainly compressional, this state has also a small toroidal fraction. In  $K=0$  channel, the toroidal strength is much weaker than in  $K=1$  case.

Altogether, figures 1 and 2 show that, in accordance with the previous studies for low-energy dipole spectra in rare-earth deformed nuclei [13, 24], the toroidal (compressional) mode dominates in  $K=1$  ( $K=0$ ) strength. In  $^{24}\text{Mg}$ , both modes exhibit a significant deformation-induced downshift. As a result, they acquire the lowest energies in their  $K$ -channels and become well separated from higher dipole states. This can essentially facilitate their experimental discrimination.

To understand the impact of deformation, it is instructive to consider the structure of the toroidal  $K=1$  7.92-MeV state and compressional  $K=0$  9.56-MeV state. Table I shows that the toroidal 7.92-MeV state is mainly formed by two (proton and neutron) 2qp components of the same content. Altogether they exhaust 93% of the states norm. In the more collective 9.56 MeV state, two

TABLE I: Properties of the lowest QRPA dipole states in  $^{24}\text{Mg}$  at  $\beta=0.536$ . The columns include: the excitation energy  $E$  (in MeV),  $K$ -value, transition rate  $B(E3K, 0_{\text{gs}}^+ \rightarrow 3^- K)$  (in W.u.), two main 2qp components (in Nilsson asymptotic quantum numbers), position (F-pos) of the single-particle levels relative to the Fermi (F) level, and contributions of 2qp components  $\mathcal{N}$  to the state norm.

$E$	$K$	$B(E3K)$	main 2qp comp	F-pos	$\mathcal{N}$
7.92	1	11.7	pp[211] $\uparrow$ -[330] $\uparrow$	F, F+4	0.54
			nn[211] $\uparrow$ -[330] $\uparrow$	F, F+4	0.39
9.56	0	17.0	pp[211] $\downarrow$ -[101] $\downarrow$	F-2, F+2	0.39
			nn[211] $\downarrow$ -[101] $\downarrow$	F-2, F+2	0.31

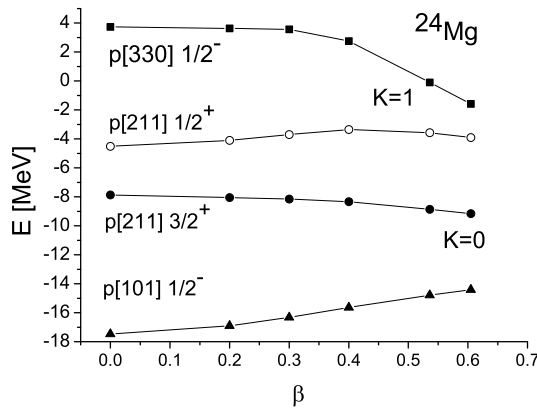


FIG. 3: Energies of proton single-particle states in  $^{24}\text{Mg}$ .

main 2qp components exhaust 70%. In both cases, the major components are quite large and so should dominate features of the states.

In figure 3, the deformation dependence of the energies of single-particle states from the major 2qp components is depicted. Only proton states are considered since in  $N=Z$  nuclei the neutron states exhibit a similar behavior. We see that, for  $\beta \geq 0.4$ , the deformation growth yields a rapid decrease of  $[330]\uparrow$ -energy, significant increase of  $[101]\downarrow$ -energy and a relatively small change of the energies for  $[211]\uparrow$  and  $[211]\downarrow$ . This leads to decrease of the energies of 2qp configurations  $\text{pp}[211]\uparrow$ -[330] $\uparrow$  and  $\text{pp}[211]\downarrow$ -[101] $\downarrow$  with  $\beta$ , which in turn explains the downshift of the toroidal and compressional modes at large deformations.

Since the energy downshift in  $^{24}\text{Mg}$  is mainly determined by the deformation dependence of particular single-particle states in near Fermi energy, this effect is not universal. In other words, TS and CS in other deformed light nuclei are not necessarily the lowest dipole states. To demonstrate this, we compare below the results for  $^{24}\text{Mg}$  with those for  $^{20}\text{Ne}$ , another  $N=Z$  nucleus with the strong quadrupole deformation.

## B. $^{20}\text{Ne}$

For  $^{20}\text{Ne}$ , our SLy6 calculations give the equilibrium deformation  $\beta=0.56$  which is considerably smaller than the experimental value  $\beta_{\text{exp}}=0.72$  [25]. Note that  $\beta_{\text{exp}}$  is determined by  $B(E20)$  transition  $I^\pi K=0^+0 \rightarrow 2^+0$  in the ground state band and so acquires large contributions from dynamical correlations, especially in soft nuclei. As a result, the obtained  $\beta_{\text{exp}}$  are allowed to be larger than the actual "static" equilibrium deformation. Below we present the responses for both axial deformations,  $\beta=0.56$  and 0.72.

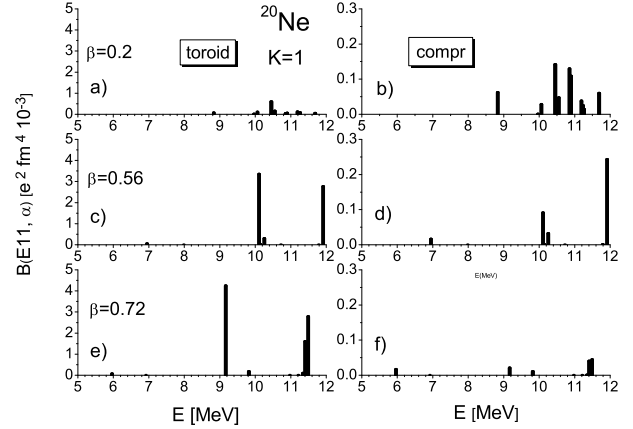


FIG. 4:  $T=0$  toroidal (left) and compressional (right)  $B(E11)$ -responses for  $K=1$  states in  $^{20}\text{Ne}$ , calculated for deformations  $\beta=0.2$  (upper), 0.56 (middle), and 0.72 (bottom). Note different scales in the left and right plots.

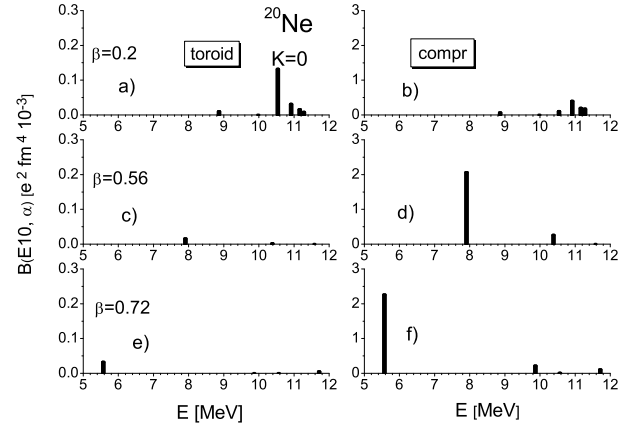


FIG. 5: The same as in Fig. 4 but for  $K=0$  states. Note different scales in the left and right plots.

Figures 4 and 5 show the toroidal and compressional responses in  $^{20}\text{Ne}$  for  $K=1$  and  $K=0$  states at deformations  $\beta=0.2$ , 0.56 and 0.72. We see that, in accordance with the results for  $^{24}\text{Mg}$ , the toroidal mode dominates in  $K=1$  strength while the compressional mode is major for  $K=0$ . The responses are peaked in certain states. At  $\beta=0.56$ , there are the strong toroidal  $K=1$  peak at 10.11 MeV and

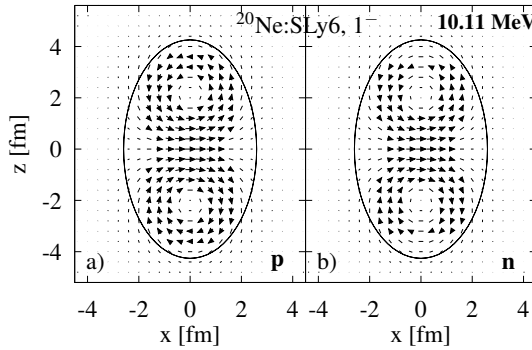


FIG. 6: Proton (left) and neutron (right) QRPA (SLy6) convective currents (CTD) in  $z$ - $x$  ( $y=0$ ) plane for the  $K=1$  10.11-MeV state in  $^{20}\text{Ne}$ . Magnitude of the currents is determined by arrow lengths in arbitrary units.

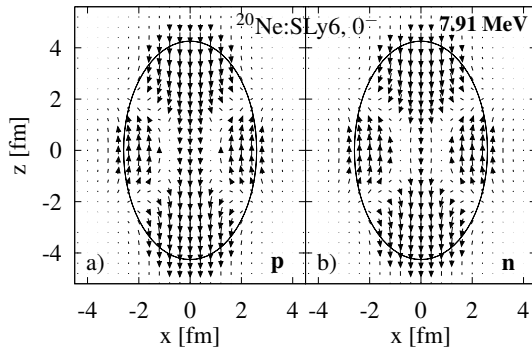


FIG. 7: The same as in Fig. 6 but for  $K=0$  7.91-MeV state.

compressional  $K=0$  peak at 7.91 MeV. The toroidal and compressional nature of these states is confirmed by the pattern of the convective current exhibited in figures 6 and 7.

Like in  $^{24}\text{Mg}$ , TS and CS in  $^{20}\text{Ne}$  also exhibit the energy downshift with  $\beta$ . However in  $^{20}\text{Ne}$ , only  $K=0$  CS becomes the lowest excitation while  $K=1$  TS is preceded by other dipole states ( $\sim 7$  and 8 MeV at  $\beta=0.56$  and  $\sim 6$  and 7 MeV at  $\beta=0.72$ ). Moreover, unlike the  $^{24}\text{Mg}$  case, the CS lies below the TS.

These results can be partly understood by inspecting the structure of the relevant states and their deformation dependence. Table II shows that, in the toroidal  $K=1$  state at 10.11 MeV and compressional  $K=0$  state at 7.91 MeV, the major proton and neutron 2qp compo-

TABLE II: The same as in Table I but for  $^{20}\text{Ne}$  at  $\beta=0.56$ . The energy  $E$  is in [MeV], the transition rate  $B(E3K)$  is W.u..

$E$	$K$	$B(E3K)$	main 2qp comp	F-pos	$\mathcal{N}$
7.91	0	45.6	pp[220] $\uparrow$ -[330] $\uparrow$	F, F+5	0.21
			nn[220] $\uparrow$ -[330] $\uparrow$	F, F+5	0.16
10.11	1	0.5	pp[220] $\uparrow$ +[330] $\uparrow$	F, F+5	0.53
			nn[220] $\uparrow$ +[330] $\uparrow$	F, F+5	0.32

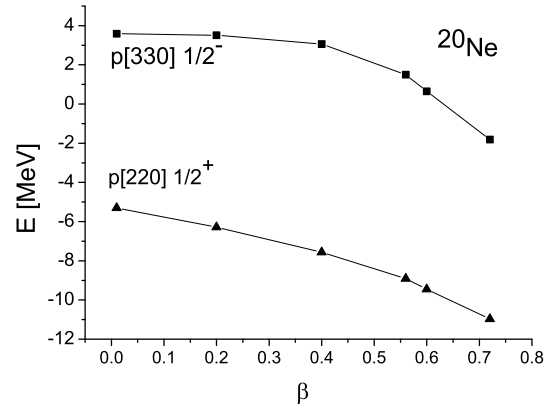


FIG. 8: The same as in Fig. 3 but for  $^{20}\text{Ne}$ .

nents embrace the same single-particle states,  $[220]\uparrow$  and  $[330]\uparrow$ . However, depending on their coupling into  $K=1$  or  $K=0$  configuration, they produce the vortical toroidal or the irrotational compressional mode. Like in  $^{24}\text{Mg}$ , the major 2qp components in TS exhaust most of the state norm (85%). This once more confirms the previous findings [26, 27] that the toroidal mode is basically of mean field origin. Instead, the compressional  $K=0$  state at 7.91 MeV is much more collective.

In our QRPA calculations, the forward amplitudes of conjugate proton and neutron 2qp components given in Tables I and II have the same sign. This complies with the isoscalar character of the low-energy TS and CS. Just in  $T=0$  case, protons and neutrons contribute constructively into toroidal or compression flows.

In figure 8, we show deformation dependence of the energies of the single-particle states  $[220]\uparrow$  and  $[330]\uparrow$  forming 2qp components in Table II. Both energies decrease with  $\beta$ . At  $\beta > 0.56$ , the energy difference for these states somewhat decreases, which partly explains the energy downshift of the TS and CS. Note that the case of the collective CS is more complicated and can hardly be treated by mere quasiparticle arguments.

It is interesting that the irrotational current for  $K=0$  CS at 7.91 MeV, given in figure 7, is similar to the octupole flow for the first  $3^-$  state in  $^{208}\text{Pb}$  [26]. Moreover, in our calculations, the  $3^-0$  rotational state built on the collective 7.91-MeV band head results in a strong E30 transition from the ground state (gs) band yielding  $B(E30, 0_{\text{gs}}^+ \rightarrow 3^-0) = 45.6$  W.u. (see Table II). The latter can be explained by collectivity of the state and by the fact that its major 2q components fully obey the selection rules for E30 transitions:  $\Delta K = 0$ ;  $\Delta N = \pm 1, \pm 3$ ;  $\Delta n_z = \pm 1, \pm 3$ ;  $\Delta \Lambda = 0$  [28]) where  $[Nn_z\Lambda]K$  are Nilsson asymptotic quantum numbers. The octupole features of the 7.91-MeV state are not surprising since in deformed nuclei the dipole and octupole excitations are coupled. One may suggest that the compressional 7.91 MeV state is actually a familiar octupole irrotational  $K=0$  state. A similar conclusion can be done for the compressional  $K=0$  9.56-MeV state in  $^{24}\text{Mg}$ .

As seen from Tables I and II, TS in  $^{24}\text{Mg}$  and  $^{20}\text{Ne}$  give very different  $B(E31)$ -values: 11.7 W.u. and 0.5 W.u., respectively. For the first glance, this is surprising since both states are non-collective and their major 2qp components exhaust nearly the same amount of the state norm. However, the difference in  $B(E3)$  can be easily understood using the selection rules for E31 transitions:  $\Delta K = \pm 1$ ;  $\Delta N = \pm 1, \pm 3$ ;  $\Delta n_z = 0, \pm 2$ ;  $\Delta \Lambda = 1$  [28]. It is easy to see that in  $^{24}\text{Mg}$  the major TS components fully obey the selection rules and so this state exhibits the large  $B(E31)$ . Instead, in  $^{20}\text{Ne}$ , the major TS components violate the rules for  $n_z$  and  $\Lambda$  and so the E31 transition is strongly suppressed.

Following Tables I and II, the conjugate proton and neutron 2qp components give similar but not precisely the same contributions to the state norm. This means that predominately isoscalar TS and CS have a minor isovector admixture. While the collective  $K=0$  CS demonstrate the octupole features, the  $K=1$  TS perhaps correspond to low-energy isoscalar dipole states (LE-IDS) found in light  $N=Z$  spherical doubly magic nuclei ( $^{16}\text{O}$ ,  $^{16}\text{Ca}$ ). LE-IDS are characterized by weak isospin-forbidden E1 transitions. They were widely explored some time ago, see early studies [29, 30] and recent detailed analysis [31]. Following [31], these states can exhibit the toroidal flow. In our calculations,  $K=1$  TS in  $^{24}\text{Mg}$  and  $^{20}\text{Ne}$  also exhibit weak dipole transitions with  $B(E1, 0^+0_{\text{g.s.}} \rightarrow 1^-1) = 2.52 10^{-4}$  and  $0.93 10^{-4} \text{ e}^2\text{fm}^2$ , respectively. Perhaps these TS represent the realization of LE-IDS in strongly deformed axial nuclei.

#### IV. CONCLUSIONS

We analyzed the influence of strong axial quadrupole deformation on the properties of individual low-energy  $E1(T=0)$  toroidal and compressional states (TS and CS) in the  $N=Z$  nuclei  $^{24}\text{Mg}$  ( $\beta_{\text{exp}}=0.605$ ) and  $^{20}\text{Ne}$  ( $\beta_{\text{exp}}=0.72$ ). The study was performed within the self-consistent quasiparticle random-phase approximation approach using the Skyrme parametrization SLy6. As shown in [1], the large quadrupole deformation in  $^{24}\text{Mg}$  causes a considerable energy downshift of TS and CS. As a result, they become the energetically lowest dipole

$K=1$  and  $K=0$  excitations. Here we explain this effect by deformation dependence of the energies of the major two-quasiparticle (2qp) components in TS and CS.

Since the downshift effect is determined by deformation properties of the particular 2qp configurations, it is not universal and in principle can differ in other light deformed nuclei. Indeed, in  $^{20}\text{Ne}$ , the deformation also yields the energy downshift of TS and CS. However, the TS is not anymore the lowest dipole state even in  $K=1$  channel. Instead CS is the lowest dipole state lying below TS. Perhaps light deformed nuclei with the lowest  $K=1$  TS are rare. To our knowledge, they are limited by  $^{24}\text{Mg}$  [1] and  $^{10}\text{Be}$  [16].

The calculation for  $^{20}\text{Ne}$  confirm the finding [1, 13, 24] that, in axially deformed nuclei, the E1 vortical toroidal strength dominates in  $K=1$  low-energy spectra while the irrotational compressional strength prevails in  $K=0$  channel. CS in  $^{20}\text{Ne}$  and  $^{24}\text{Mg}$  are collective and remind familiar low-energy collective E30 octupole modes pertinent to deformed nuclei where dipole and octupole excitations are mixed. Instead, TS are mainly formed by two large conjugate proton and neutron 2qp components. So the toroidal flow is basically of mean-field origin. Perhaps TS in  $^{20}\text{Ne}$  and  $^{24}\text{Mg}$  correspond to low-energy  $T=0$  dipole states with the isospin-forbidden E1 transitions, which were earlier discussed for  $N=Z$  doubly-magic nuclei [29–31]. The TS could be a realization of such states in strongly deformed nuclei. We plan to consider this point in next studies.

V.O.N. thanks Profs. P. von Neumann-Cosel, J. Wambach and V.Yu. Ponomarev for valuable discussions. The work was partly supported by the Heisenberg - Landau (Germany - BLTP JINR), and Votruba - Blokhintsev (Czech Republic - BLTP JINR) grants. A.R. is grateful for support from Slovak Research and Development Agency (Contract No. APVV-15-0225) and Slovak grant agency VEGA (Contract No. 2/0129/17). J.K. appreciates the support of the research plan MSM 0021620859 (Ministry of Education of the Czech Republic) and the Czech Science Foundation project P203-13-07117S.

- 
- [1] V.O. Nesterenko, A. Repko, J. Kasil, and P.-G. Reinhard, Phys. Rev. Lett. **120**, 182501 (2018).  
 [2] S. F. Semenko, Sov. J. Nucl. Phys. **34**, 356 (1981).  
 [3] S. I. Bastrukov, Š. Mišicu, and A. V. Sushkov, Nucl. Phys. A **562**, 191 (1993).  
 [4] Š. Mišicu, Phys. Rev. C **73**, 024301 (2006).  
 [5] N. Ryezayeva et al, Phys. Rev. Lett. **89**, 272502 (2002).  
 [6] G. Colo, N. Van Giai, P. F. Bortignon, and M. R. Quaglia, Phys. Lett. B **485**, 362 (2000).  
 [7] D. Vretenar, N. Paar, P. Ring, and T. Nikšić, Phys. Rev. C **65**, 021301(R) (2002).  
 [8] N. Paar, D. Vretenar, E. Kyan, G. Colo, Rep. Prog. Phys. **70**, 691 (2007).  
 [9] J. Kvasil, V. O. Nesterenko, W. Kleinig, P.-G. Reinhard, and P. Vesely, Phys. Rev. C **84**, 034303 (2011).  
 [10] A. Repko, P.-G. Reinhard, V. O. Nesterenko, and J. Kvasil, Phys. Rev. C **87**, 024305 (2013).  
 [11] P.-G. Reinhard, V. O. Nesterenko, A. Repko, and J. Kvasil, Phys. Rev. C **89**, 024321 (2014).  
 [12] V.O. Nesterenko, J. Kvasil, A. Repko, W. Kleinig, P.-G. Reinhard, Phys. Atom. Nucl. **79**, 842 (2016).  
 [13] A. Repko, J. Kvasil, V. O. Nesterenko, and P.-G. Rein-

- hard, Eur. Phys. J. A **53**, 221 (2017).
- [14] D. H. Youngblood, Y.-W. Lui, B. John, Y. Tokimoto, H. L. Clark, and X. Chen, Phys. Rev. C **69**, 054312 (2004).
- [15] M. Uchida, et al, Phys. Rev. C **69**, 051301(R) (2004).
- [16] Y. Kanada-Enyo and Y. Shikata, Phys. Rev. C **95**, 064319 (2017).
- [17] M. Bender, P.-H. Heenen, and P.-G. Reinhard, Rev. Mod. Phys. **75**, 121 (2003).
- [18] E. Chabanat, P. Bonche, P. Haensel, J. Meyer, and R. Schaeffer, Nucl. Phys. A**635**, 231 (1998).
- [19] A. Repko, J. Kvasil, V. O. Nesterenko, and P.-G. Reinhard, arXiv:1510.01248[nucl-th].
- [20] P. Ring and P. Schuck, *The Nuclear Many-Body Problem* (Springer-Verlag, Berlin, 1980).
- [21] V. O. Nesterenko, W. Kleinig, J. Kvasil, P. Vesely, and P.-G. Reinhard, Int. J. Mod. Phys. E **17**, 89 (2008).
- [22] M. N. Harakeh and A. van der Woude, *Giant Resonances* (Clarendon Press, Oxford, 2001).
- [23] A. Repko, J. Kvasil, and V. O. Nesterenko, under preparation for publication.
- [24] J. Kvasil, V. O. Nesterenko, W. Kleinig, and P.-G. Reinhard, Phys. Scr., **89**, 054023 (2014).
- [25] Database <http://www.nndc.bnl.gov>.
- [26] D. G. Ravenhall and J. Wambach, Nucl. Phys. A **475**, 468 (1987).
- [27] V.O. Nesterenko, A. Repko, P.-G. Reinhard, and J. Kvasil, EPJ Web of Conferences, **93**, 01020 (2015).
- [28] S.G. Nilsson, Mat. Fys. Medd. Dan. Vid. Selsk. **29**, n.16 (1965).
- [29] H. Miska, H.D. Gräf, A. Richter, D. Schüll, E. Spamer and O. Titze, Phys. Lett. B **59**, 441 (1975).
- [30] B. Castel, Y. Okuhara, and H. Sagawa, Phys. Rev. C **42**, R1203 (1990).
- [31] P. Papakonstantinou, V.Yu. Ponomarev, R. Roth, and J. Wambach, Eur. Phys. J. A **47**, 14 (2011).